Industrial Crops & Products 147 (2020) 112168

Contents lists available at ScienceDirect

Industrial Crops & Products

journal homepage: www.elsevier.com/locate/indcrop

RNA-Seq transcriptome analysis of *Jatropha curcas* L. accessions after salt stimulus and unigene-derived microsatellite mining

Marislane Carvalho Paz de Souza[a], Manassés Daniel da Silva[a], Eliseu Binneck[b], George André de Lima Cabral[a], Ana Maria Benko Iseppon[a], Marcelo Francisco Pompelli[c], Laurício Endres[d], Éderson Akio Kido[a,*]

[a] Federal University of Pernambuco (UFPE), Bioscience Center, Department of Genetics, 50670-420 Recife, PE, Brazil
[b] Brazilian Agricultural Research Corporation (EMBRAPA), EMBRAPA-Soybean, 86001970 Londrina, PR, Brazil
[c] Federal University of Pernambuco (UFPE), Bioscience Center, Department of Botany, 50670-901 Recife, PE, Brazil
[d] Federal University of Alagoas (UFAL), Agricultural Sciences Center, 57072-970 Maceió, AL, Brazil

ARTICLE INFO

Keywords:
Bioinformatic
Abiotic stress
Euphorbiaceae
Physic nut

ABSTRACT

The small oleaginous tree of *Jatropha curcas* L. (physic nut) is an excellent biodiesel source whose crop could represent a good income source for farmers in tropical and semi-arid zones. However, in some areas in particular, salinity, such as many other abiotic stresses, can compromise productivity. We analyzed the root RNA-Seq transcriptome of two Brazilian *J. curcas* accessions after a three-hour NaCl exposition (150 mM) aiming at identifying differentially expressed genes (DEGs) useful for breeding programs. The *de novo* transcriptome covered 145,422 assembled transcripts (126,343 unigenes), out of which 84,589 showed at least one significant alignment to the GenBank reference genome. Differentially expressed unigenes (DEGs) of the salt-sensitive Jc171 accession (4,646) suppressed those of the salt-tolerant Jc183 (57) one. A MapMan analysis of the DEGs using *Manihot esculenta* Crantz genes as reference (Euphorbiaceae family) highlighted the metabolism of phytohormone, carbohydrate (CHO), lipid, amino acid, redox, and secondary metabolite in the salt-responses. RT-qPCR results of nine selected Jc183 DEGs [phenylalanine ammonia-lyase (*PAL*), S-adenosylmethionine-dependent methyltransferase (*SAMe*), S-adenosylmethionine synthase (*SAM*), carboxylesterase (*CXE*), homeobox-leucine zipper gene (*HD-Zip*), NAC transcription factor gene (*NAC*), methionine-gamma lyase (*MGL*), peroxidase (*PX*), and xyloglucan endotransglucosylase (*XTH*)] evaluated in 36 combinations accession/treatments validated 86.11 % of the *in silico* results. The data generated improved the *J. curcas* transcriptome based on Illumina-21 bp tags as reported before, which can benefit breeders in the improvement of salt-tolerance in *J. curcas*. Additionally, primer pairs successfully designed for 1,423 DEGs presenting microsatellite motifs can contribute to the development of co-dominant molecular markers, a very useful marker applied to genetic analysis.

1. Introduction

The physic nut (*Jatropha curcas* L.) is an oilseed plant from the Euphorbiaceae family widely distributed throughout tropical and semiarid regions (Africa, Asia, and South America). Its occurrence combines different climates and soil conditions, including marginal agricultural and nutritionally deficient areas (Wang et al., 2018; Beltrão and Oliveira, 2008). *J. curcas* seeds have high oil contents (40–50 %) and a relatively high amount of unsaturated fatty acids, thus representing a suitable choice for the biodiesel industry (Pramanik, 2003; Grover et al., 2014). In Brazil, biodiesel production has increased over the past decade as a result from soybean oil processing. However, the versatile crop of soybean is very significant to both human and animal nutrition. In contrast, the food market does not benefit from *J. curcas*, which makes it a possible option for exploration as a biodiesel resource. Despite its relatively drought-tolerant nature, *J. curcas* is a salt-sensitive plant. Soil salinity is known as a major cause of losses in agricultural production worldwide (FAO, 2015). Globally, it is estimated that 20 % of all irrigated land is affected by salt stress (Taiz et al., 2017). Several factors, including soil composition, poor drainage, and inadequate irrigation, may provoke salt stress, and their combination makes the Brazilian Northeast region potentially sensitive to salinity.

Plants in saline soils may grow irregularly due to the osmotic stress caused by the reduced water absorption. In addition, the high ion

* Corresponding author.
E-mail address: ederson.kido@ufpe.br (É.A. Kido).

https://doi.org/10.1016/j.indcrop.2020.112168
Received 30 April 2019; Received in revised form 23 January 2020; Accepted 24 January 2020
Available online 15 February 2020

concentration interfering with the nutrient uptake may cause cytotoxicity (Munns, 2005). Understanding the molecular mechanisms through which plants respond to salt stress is crucial to plant breeding programs. Therefore, it is useful to compare gene expression profiles of accessions with different responses to NaCl in order to identify genes related to salt tolerance. Transcriptomic approaches have been applied to *J. curcas* plants in response to abiotic stresses, including low temperatures (Wang et al., 2013, 2014), flooding (Juntawong et al., 2014), drought (Cartagena et al., 2015; Sapeta et al., 2015; Zhang et al., 2015), and salinity (Zhang et al., 2014). Zhang et al. (2014) reported transcriptomic data regarding salinity comprising Illumina 21 bp tags from roots and leaves of the cultivar GZQX0401 (eight-week germination), exposed to 100 mM NaCl for periods of two hours, two days, and seven days. This cultivar is the inbred line whose genome is the GenBank reference (GCA_000696525.1). The authors observed more regulated genes in the roots detected 2 h after the stress, surpassing those detected after two days. In this study, we exposed plants of two Brazilian *J. curcas* accessions that had been germinated ten weeks earlier and had contrasting salt-response to 150 mM NaCl during three hours. The root samples allowed to generate the RNA-Seq transcriptome, whose analysis provided insights on the metabolic strategies of plants responding to salinity. Additionally, a set of successfully designed primers targeting differentially expressed transcripts presenting microsatellite motifs could benefit breeders to develop co-dominant molecular markers, a very useful tool in genetic analysis.

2. Materials and methods

2.1. Plant materials and the NaCl assay

We selected the two *J. curcas* Brazilian accessions with contrasting salt-responses (Jc183 and Jc171) based on the work by Lozano-Isla et al. (2018). We carried out the salt-stress assay in the greenhouse of the Laboratory of Plant Physiology at the Federal University of Alagoas (-9°27′55″, -35°49′31″; 130 m a.s.l., Maceio, AL, Brazil. The regional climate is classified as "Am," i.e., tropical monsoon climate according to the Köppen classification (Peel et al., 2007), with 1,523 ± 383.4 mm of total annual rainfall scattered throughout the year (Proclima, 2019). During the assay, an automatic weather station (model WS-GP1; DELTA-T Devices, Cambridge, England) monitored the environmental conditions inside the greenhouse, including temperature and relative air humidity (recorded every 5 min). We calculated the vapor pressure deficit (VPD) based on temperature and relative humidity data. Additionally, pyranometers (mod. LI-200R, Li-Cor, Lincoln, NE, USA) measured the photosynthetically active radiation (PAR) at 10 s intervals. For the salinity assay, seeds of both accessions were subjected to a 20 min disinfection using a NaOCl 2 % (v/v) solution containing two drops of Tween 20™ and sterile deionized water rinsing for three consecutive times. The disinfected seeds germinate in polypropylene trays (50 × 30 × 10 cm) until the first-leaf expansion (around 15 days after germination, DAG) with the plantlets receiving only water. Subsequently, we transplanted the seedlings (March 2016) to pots (50 L) containing washed sand (20 kg). The experimental salt assay followed a completely randomized design with two accessions, two treatments (without salt or with NaCl, 150 mM, three-hour salt exposure), and three plants of each accession simulating biological replicates. We irrigated the plants every three days using Hoagland nutrient solution (Hoagland and Arnon, 1950) with one-fifth strength. Seven days before the salt application (62 DAG), we irrigated plants daily with full-strength Hoagland nutrient solution. On the day before the salt application, plants were irrigated at 16 p.m. We applied the salt at nine a.m., which consisted of NaCl added to the Hoagland solution (final concentration: 150 mM). After a three-hour salt exposition, we collected the roots to be immediately frozen in liquid nitrogen and stored (−80 °C) until RNA extraction.

2.2. RNA extraction and RNA-Seq libraries

We extracted the total RNAs from roots by following the instructions in the SV Total RNA Isolation kit (Promega Corp., USA) and verified the RNAs integrities using RNA agarose gel (1.5 % w/v), while the RNAs concentrations were estimated in NanoDrop® 2000 spectrophotometer (Thermo Scientific ™). RNAs indicating an absorbance ratio 260/280 nm close to 2.0 and a minimum of 50 µL RNA solution (80 ng/µL) were sent to ESALQ – Genomic Center (São Paulo University, Piracicaba, SP, Brazil) to generate and sequence the RNA-Seq libraries. We reassessed all the RNAs integrities using an Agilent 6000 Bioanalyzer (Agilent Technologies, CA, USA). The generation of a total of 12 RNA-Seq libraries (two accessions x two treatments x three plants each accession) followed the LS protocol of the Illumina TruSeq Stranded mRNA Sample Prep kit (Illumina, Inc, CA, USA). Libraries were sequenced on an Illumina HiSeq 2500 (paired-end 100 bp reads) using flow Cell HiSeq run with the HiSeq SBS v4 chemistry.

2.3. De novo transcriptome assembly and differentially expressed genes identification

We analyzed the RNA-Seq raw data (FastQC v0.11.5) for sequence read quality before and after the initial filtering and trimming using the default parameters of the Trimmomatic tool (v.0.36; Bolger et al., 2014). Reads showing low quality or unknown adapters and nucleotides were excluded. Pairs of high-quality reads (Phred quality score, $Q \geq 30$ for all bases) were used for *de novo* transcriptome assembly performed on the Trinity software v.2.2.0 (Grabherr et al., 2011). A de Bruijn graph data structure displayed the overlaps among the reads, and short reads with overlapping regions were assembled into longer contigs. The longest transcripts in the cluster units were considered unigenes to eliminate redundant sequences. We used the alignment package Bowtie (v4.4.7; Langmead et al., 2009) to map reads back into unigenes. According to the comparison results, RSEM (RNA-Seq through expectation maximization; Li and Dewey, 2011) estimated the expression levels. The fragments per kilobase of transcript per million mapped reads (FPKM) represented the differences in the unigene expression abundance among the samples. We used matrices of normalized FPKM values generated from the RSEM package for the differential expression analyses between the experimental conditions using the edgeR package (Robinson et al., 2010). Differentially expressed (uni) genes (DEGs) considered the *p-value* ≤ 0.0001, the false discovery rate (FDR ≤ 0.005), and the fold change (FC) values based on Log_2 (FC) ≥ 1 (positive expression modulation or up-regulation, UR) or $\leq$ -1 (negative modulation or down-regulation, DR). FC values represented the ratio of the unigene abundance considering their presence in two compared RNA-Seq libraries. We analyzed the quality of the transcriptome assembly on the rnaQUAST-1.5.2 software (Bushmanova et al., 2016) by applying the *J. curcas* reference genome from the GenBank (accession GCA_000696525.1) and default parameters.

2.4. Functional annotation of the assembled transcripts

We annotated the assembled transcripts by using BLASTx alignment (e-value $\leq 10^{-10}$) to different protein databases, including *J. curcas* (UniProtKB; http://www.uniprot.org/), *Manihot esculenta*, and *Ricinus comunnis* L. (*Phytozome* v.12.1.6; https://phytozome.jgi.doe.gov/pz/portal.html). The contribution of each dataset was detected through Venn diagrams (Oliveros, 2015). We performed (BLASTx, e-value $\leq 10^{-5}$) a second round of functional annotation, containing the Trinotate pipeline (https://trinotate.github.io/), against several databases, including: NCBI (nr protein database; ftp://ftp.ncbi.nih.gov/blast/db/), UniProt/SwissProt database, Kyoto Encyclopedia of Genes and Genomes (KEGG), eggNOG, and InterproScan. Trinotate also provided a web-based graphical interface to support local user-based navigation of annotations and differential expression data (Bryant et al., 2017).

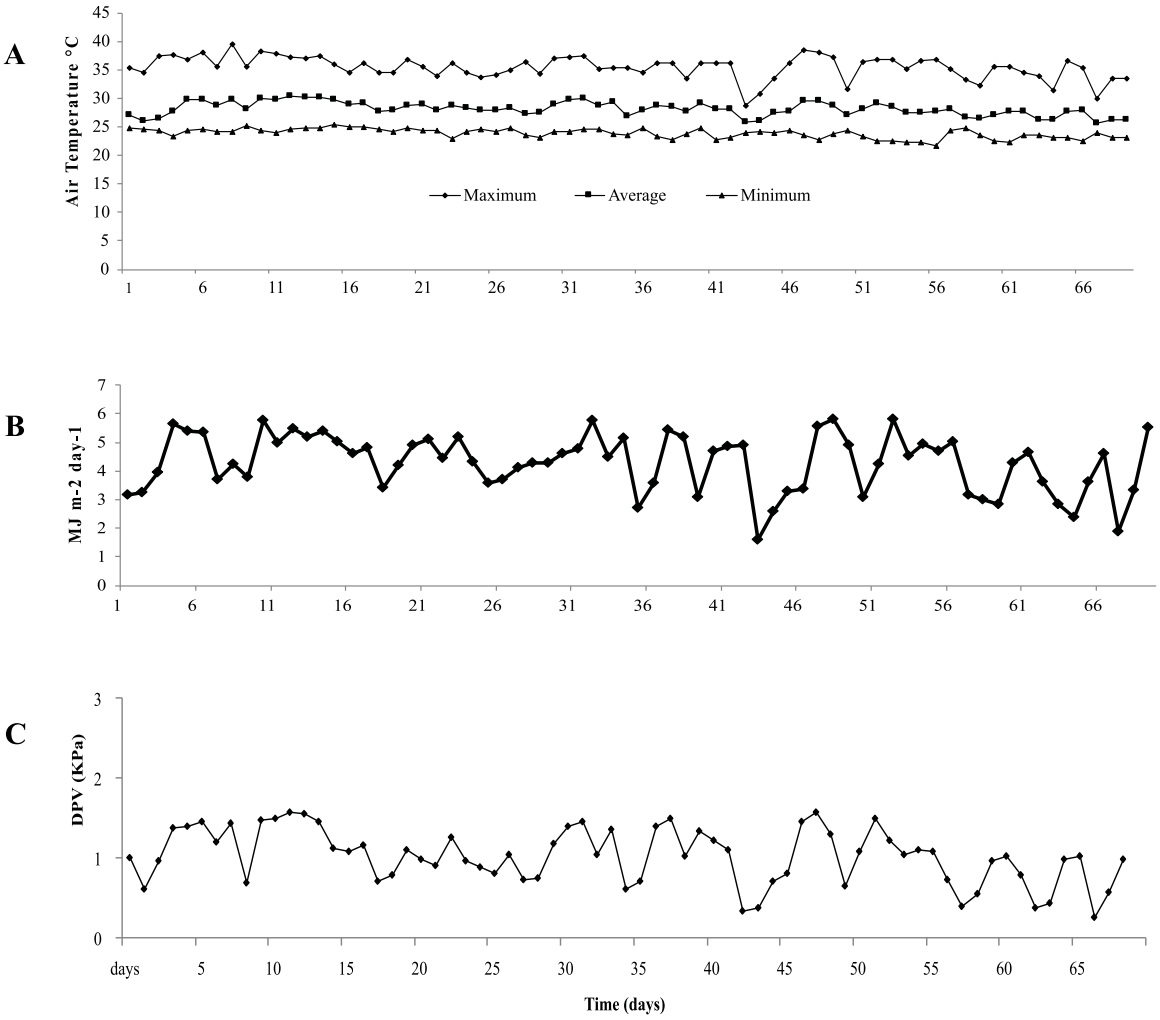

Fig. 1. Environmental data recorded inside the greenhouse and during the experimental assay period with *Jatropha curcas* plants before the salt-treatment (the last day correspond to the day of the salt stress application): (A) Minimum, average and maximum temperature, °C, (B) photosynthetically active radiation (PAR, average, MJ m^{-2} day^{-1}), and (C) vapor pressure deficit (DPV, average, KPa).

2.5. Metabolic pathways, and heatmaps

The MapMan software (v.3.6.0; Thimm et al., 2004) identified the metabolic pathways associated with DEGs after the application of the *M. esculenta* best hits from the BLAST alignments. In the Euphorbiaceae family, *M. esculenta* is the only species previously associated with the MapMan bin codes and their sequences were used as reference. We generated the hierarchical clustering of the unigenes and DEGs on the Cluster software (v.3.0; https://cluster2.software.informer.com/3.0/) based on FC values considering the ratio of frequencies in the stressed *versus* the respective negative control library. The clusters were visualized as heatmaps on the Java Treeview software (v.1.1; Saldanha, 2004).

2.6. Expression validation by RT-qPCR assay

The RT-qPCR analysis comprised DEGs showing relevant functional annotation in plant abiotic stress responses, according to the scientific literature, in addition to the up-expression detected in the Jc183 profile in relation to the negative control. For this purpose, we conducted a real-time assessment of the cDNAs from RNAs pre-treated with DNase using a PCR Thermocycler LineGene 9600 (Bioer, Hangzhou, China) regarding reactions including "biological" and technical triplicates for each treatment, negative controls, and two reference genes [*Actin* (Tang et al., 2016), and *β-tubulin* (Xu et al., 2016)], properly tested to this end. We also designed (Primer3 tool; Rozen and Skaletsky, 2000) *primer* pairs proposed to amplify DEGs (Table S1) based on the *J. curcas* transcripts according to the following parameters: amplicon size (70–200 bp), melting temperature [50–80 °C, 70 °C (optimum)], and GC content (45–55 %). The synthesized *primers* (Life Technologies, USA) firstly amplified cDNAs through a conventional PCR test and subsequently the RT-qPCR reactions (10 µL) included: 1 µL cDNA (sample diluted 1/5), five µL SYBR® Green (GoTaq® qPCR Master Mix, Promega), 0.3 µL of each *primer* (5 µM), and 3.4 µL ddH_2O. Reactions performed according to the following settings: initial 2 min denaturation of 95 °C followed by 40 cycles of 95 °C for 15 s, and 60 °C for 60 s. We obtained the dissociation curves by heating the amplicons from 65 to 95 °C for 20 min after the RT-qPCR cycles. The LineGene software (v.1.1.10) estimated the Tm and Cq values, as well as the absolute and relative quantifications. The relative expression data assessment was conducted on the REST 2009 software (Relative Expression Software Tool v.2.0.13; Pfaffl et al., 2002) with the application of a randomization test with 10,000 permutations; in addition to testing the hypothesis of significant differences between the control and treatment groups. In order to increase the reliabilities of the qPCR results, we followed the MIQE protocol (*The Minimum Information for Publication of Quantitative Real-Time PCR Experiments*; Bustin et al., 2009).

2.7. Microsatellite mining and primer design based on differentially expressed unigenes

We prospected the microsatellites or simple sequence repeat (SSR) motifs from *J. curcas* DEGs on the BatchPrimer3 v1.0 software (You et al., 2008). The SSR length comprised at least 12 nucleotides involving motif length of di-nucleotide (di-) to hexa-nucleotide (hexa-) with the minimum number of motif repeats presenting six (di-), four (tri-), or three (tetra-, penta-, and hexa-nucleotide). The SSR primers were collected from the SSR-flanking regions of the DEGs by applying the incorporated tool and default parameters.

3. Results

3.1. Visible damages on leaves of the Jc171 accession

During the experimental assay, we recorded 383.7 mm of rainfall with a potential evapotranspiration of 3.0 ± 0.8 mm; relative humidity varying from 65.4%–97.2 %; mean daily temperatures ranging from 25.5 °C to 30.4 °C, and global radiation intercepted by the plants reaching 5.82 MJ m^{-2} day^{-1}. On the day of salt application, the average daytime air temperature reached 27.93 °C with a vapor pressure deficit (VPD) of 0.99 K Pa; in addition, the integrated global radiation over 24 h indicated 5.50 MJ.m^{-2}.day^{-1}. Since these parameter values remained within the range of the days before the salt application (Fig. 1), we considered the *J. curcas* plants in their steady-state condition.

However, 3 h after the salt exposure (150 mM NaCl), the salt-sensitive Jc171 accession presented visible symptoms on leaves, which did not occur for the salt-tolerant Jc183, including leaves slightly curved, wilted looking, and brown colored areas on the edges progressing to necrosis (Fig. 2).

3.2. The de novo Jatropha curcas transcriptome

The 12 RNA-Seq libraries generated with high-qualities RNAs (RIN > 9, Fig. S1) after Illumina sequencing resulted in similar amounts of raw reads through accession [113,668,090 (Jc183) and 124,618,733 (Jc171)]. After the filtering and trimming of adapters and low-quality bases, reads of good quality values (*Phred score* > 30) comprised 96.9 % (Jc183) and 96.3 % (Jc171) of the total amount. Table S2 indicates the total reads per library, before and after the trimming step. The proposed *de novo* transcriptome covered 101 MB (77 MB, based on the unigenes) and 145,422 assembled transcripts (126,343 unigenes) with a GC content of 41.55 %. The N50 for transcripts reached 1,308 bp (993 pb for unigenes), which is the maximum length for at least 50 % of the total assembled sequences in contigs of that length, at least. Table S3 shows further details on the *de novo* transcriptome. A comparison of the assembly accuracy of the *de novo* transcriptome and the *J. curcas* reference genome (GenBank assembly accession GCA_000696525.1) revealed 84,534 transcripts with at least one significant alignment to the reference genome, in addition to 81,567 uniquely aligned transcripts. The average aligned fraction was 0.97, which is defined as the total number of aligned bases in the transcript divided by the total transcript length. The average of aligned bases per transcript was 910.66, while the average of single nucleotide differences with the reference genome per transcript was 2.38 (Table S4).

3.3. Functional annotation of the assembled transcripts

The first annotation round explored proteins of *J. curcas* (27,650 sequences), *M. esculenta* (41,381), and *R. comunnis* (31,221) through an independent BLASTx analysis (*e-value* ≤ e^{-10}). A total of 27,361 transcripts encoded proteins predicted for Euphorbiaceae species. Specifically, 25,668 transcripts were directly associated with the *J. curcas* proteins, while the remaining 1,693 ones associated with proteins only from the related species (Fig. 3A). Transcripts encoding proteins covering the three species ranged 19,508 (Fig. 3A). Out of the 25,668 transcripts associated with the *J. curcas* proteins, only 9,416 (Fig. 3B) were properly annotated including the protein name or gene function. From the two related species, the remaining 14,642 transcripts received adequate annotation (Fig. 3B). The contribution of *R. cumunnis* in the annotation process exceeded that of *M. esculenta* (Fig. 3B).

The second annotation round, applying the Trinotate pipeline and several databases, identified 63,079 transcripts encoding predicted proteins basically from UniProt/SwissProt (62,278 transcripts), eggNOG (42,121), and KEGG (46,013). The individual contribution of each database (Fig. 3C) highlighted the Uniprot/SwissProt contribution (through manually cured sequences). However, 82,343 transcripts did not reach the similarity threshold (*e-value* ≤ e^{-05}). Comparing the two annotation rounds, some of the 83,343 transcripts failing to hit the II round thresholdhad been previously annotated for *J. curcas* or its related species (I round), but 80,921 remained non-associated (*transcripts without similarity* – TWS II, Fig. 3D). When disregarding the transcripts showing acceptable similarities with the *J. curcas* and related species (probably non-annotated), 78,220 transcripts remained without reaching the threshold (Fig. 3E). Fig. 3F illustrates the individual and overlapped contribution of the two annotation rounds. In addition to the 24,058 (21,835 + 2,223) transcripts annotated through the I round

A B

Fig. 2. Aspects of *Jatropha curcas* leaves after three hours of exposition to Hoagland nutrient solution with NaCl (150 mM). A) Both accessions: the salt-sensitive Jc171 (blue ribbon) and the salt-tolerant Jc183 (red ribbon) accession. B) Leaves (Jc171) with visible damages: browning at the edges and brown spots.

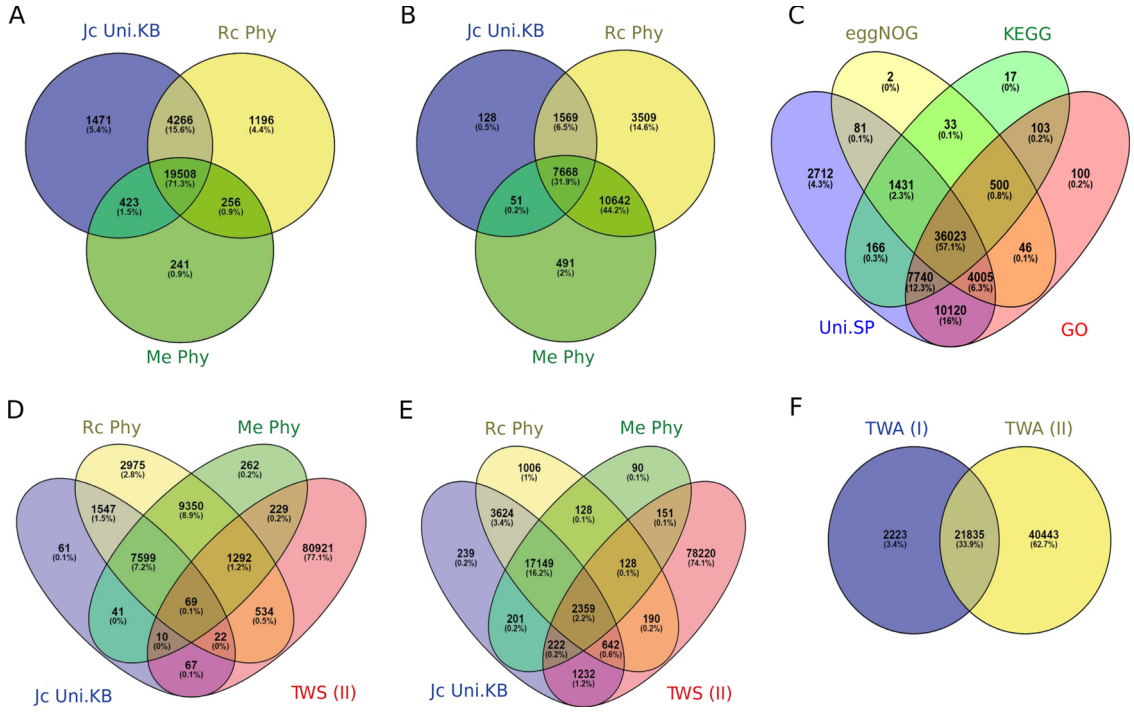

Fig. 3. Venn diagrams comparing two rounds of RNA-Seq transcript annotation: (I) applying BLASTx (*e-value* $\leq e^{-10}$) against proteins of *Jatropha curcas* L./UniProtKB (Jc UniP), *Ricinus communis* L./Phytozome (Rc Phy) and *Manihot esculenta* Crantz /Phytozome (Me Phy); (II) performing the Trinotate tool (*e-value* $\leq e^{-5}$) against several protein databases (UniProt/SwissProt, KEGG, eggNOG, GO). A) The individual and shared contribution of the datasets in the I round, based on similarities results. B) The same described in (A), but only considered the adequate annotations. C) The individual and shared contribution of the datasets in the II round. D) Transcripts encoding similar proteins to those from the I round, with or without functional annotation, when compared with transcripts without similarities from the II round (TWS II). E) Transcripts annotated (I round) compared with transcripts without similarities from the II round (TWS II). F) Transcripts with annotation (TWA) after the two annotation rounds.

analysis with Euphorbiaceae family members, other 40,443 transcripts were annotated through the II round analysis (Fig. 3F). In total, 64,501 transcripts received proper annotation, while 80,921 did not (with 78,220 having not reached the similarity threshold after two annotation rounds). Both sets represent prospective objects for further studies.

3.4. The differentially expressed unigenes in response to the salt stimulus

Regarding the gene expression data of Jc183 and Jc171, the DEG thresholds (*p-value* $\leq$ 0.0001, FDR $\leq$ 0.005, Log_2 FC $\geq$ 1 or $\leq$ -1) identified 57 and 4,646 DEGs, respectively. Among the Jc183 DEGs (40 UR and 17 DR), 23 (13 UR and 10 DR) could only be detected from the tolerant profile (five non-annotated: three UR and two DR), while 34 could be detected from the sensitive Jc171 profile as well. Of these shared DEGs, 33 presented the same regulation in both profiles (27 UR and six DR), in addition to only one divergence [DR (Jc183) and UR (Jc171) for *Galactinol synthase 1*]. Still, in the set of shared DEGs, five remained non-annotated (four UR and one DR). From the DEGs detected only in the Jc171 profile (2,753 UR and 1,859 DR), 1,296 UR remained non-annotated. Tables S5 and S6 present the details on the Jc183 and Jc171 DEGs, respectively, including id/unigene, nt/sequence, annotation, regulation, and Log_2FC.

3.5. Microsatellite mining on differentially expressed unigenes

Microsatellite or SSR mining in DEGs of Jc171 and Jc183 identified 2,427 motifs (2,405 and 22, respectively). Most of the identified motifs from Jc171 DEGs were tri- 1032, followed by tetra- 534, di- 516, penta- 181 and hexa-nucleotide 142. The motifs detected in Jc183 DEGs comprised eight di-, five tri-, four tetra-, four penta-, and one hexa-nucleotide. Table S7 indicates the SSR basic statistics. In turn, the DEGs presenting SSR motif containing successfully designed primer pairs aiming at amplifying potential SSR markers from *J. curcas* cDNAs was 1,423 (1,418/Jc171 and 14/Jc183), in which nine were common to both sets. Table S8 indicates the designed primers.

3.6. Metabolic responses of the accessions to the salt stimulus

A MapMan analysis covering more than half of all detected DEGs comprised 2,749 DEGs, including 15/Jc183 (eight UR and seven DR), 2,711/Jc171 (1,338 UR and 1,373 DR), and 23 common to both profiles, 18 UR and five DR. These DEGs were represented by *M. esculenta* best hits from the BLAST alignments. *M. esculenta* is the Euphorbiaceae species presenting data previously associated with the MapMan bin codes (Thimm et al., 2004). Table S9 presents the MapMan data associating DEGs to metabolism pathways. The hierarchical clustering of DEGs covering the metabolism of phytohormone, CHO, amino acid, lipid, redox, and secondary metabolism presented two general features (Fig. 4): a) two clusters, one grouping co-expressed unigenes increasing their abundances after the salt stimulus, and another grouping the unigenes indicating the opposite modulation; b) a more expressive gene modulation through Jc171 accession in response to the salt stimulus in relation to the Jc183 accession. Some specific results included:

- phytohormone metabolism (Fig. 4A): 58 unigenes (most of them UR) related to abscisic acid (ABA), ethylene (ETH), auxin (AUX), jasmonic acid (JA), brassinosteroids (BR), gibberellin (GA), and salicylic acid (SA);
- carbohydrate (CHO) metabolism (Fig. 4B): 32 unigenes covered the major and minor CHO metabolism; in the sucrose synthesis, the sucrose-phosphate synthase was associated with Jc171 DEG (DR, bin 2.1.1.1), and in the starch synthesis, the starch synthase was related to UR DEG (both accessions);
- amino acid metabolism (Fig. 4C): 15 unigenes related to amino acid

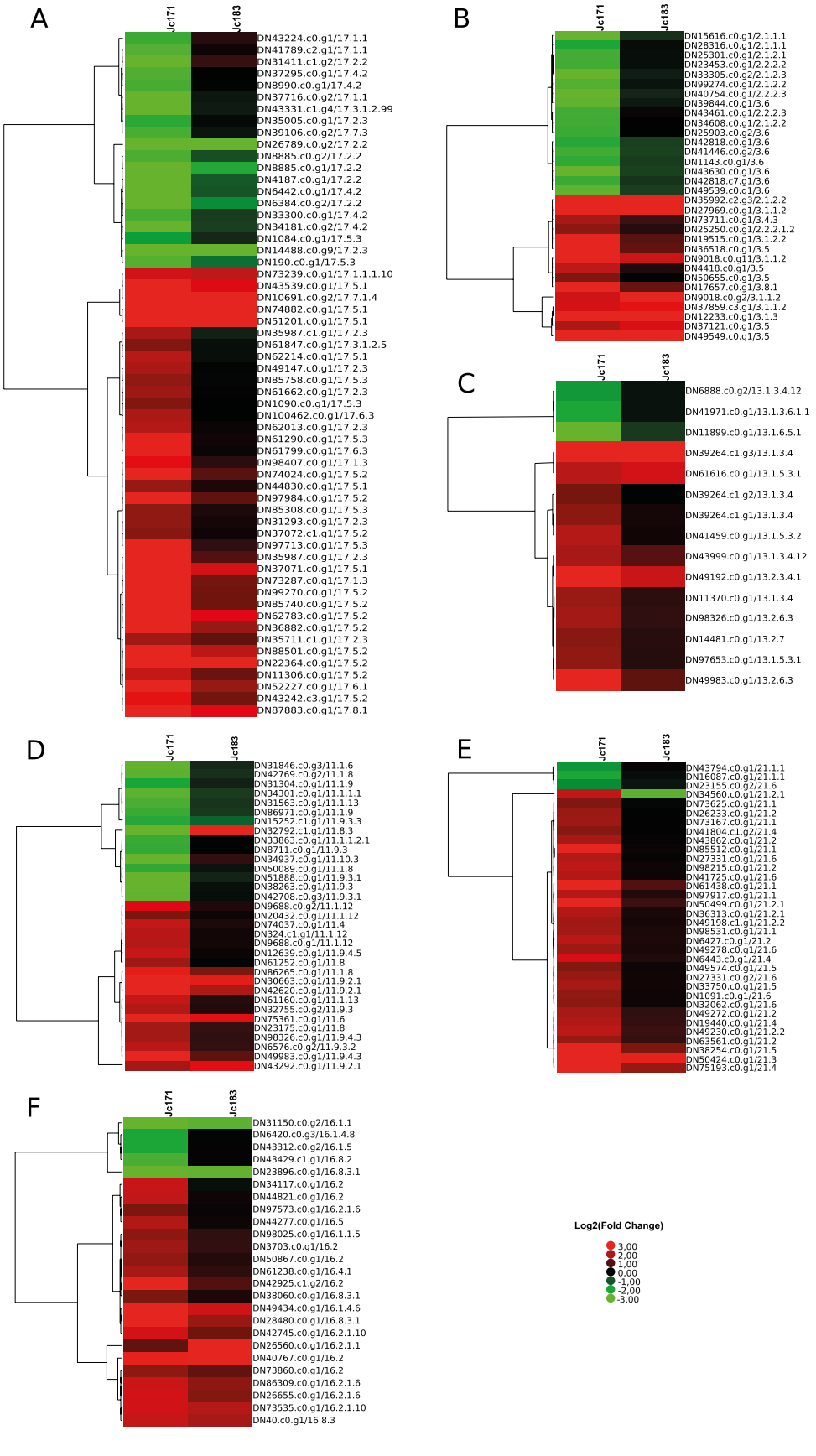

Fig. 4. Heatmaps presenting hierarchical clustering analysis, based on gene expression of Jc171 and Jc183 accessions, and different metabolisms: A) phytohormone; B) carbohydrate; C) amino acid; D) lipid; E) redox; F) secondary metabolites. Columns represent the ratio of Log_2FC (Fold Change) values, concerning the abundances of the transcript in the stressed library with the negative control library. Rows represent RNA-Seq transcripts and the respective MapMan bin codes. Clusters are on the left side. The up- or down-expression of transcripts are in red or green, respectively, and the color intensities varying based on the legend. Descriptions of the bin codes are in Table S9.

synthesis or degradation; in the cysteine biosynthesis, cysteine synthase, also O-acetyl-serine (thiol) lyase (OASTL, bin 13.1.5.3.1) and serine acetyltransferase (SAT, bin 13.1.5.3.2) were associated to UR DEGs; in the isoleucine biosynthesis, the UR DEG encoding methionine gamma-lyase (MGL; bin 13.2.3.4.1) was selected to the RT-qPCR assay;

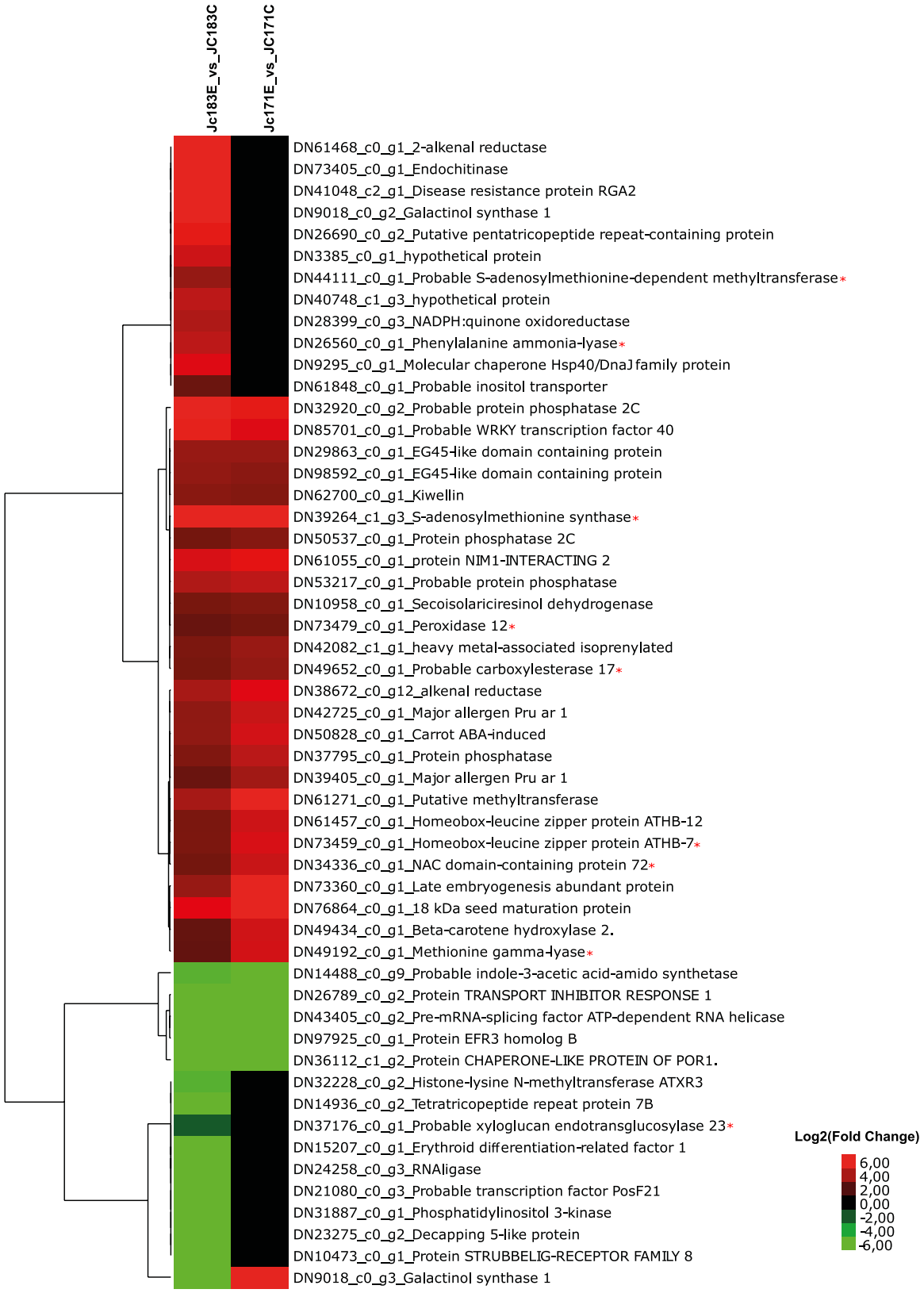

Fig. 5. Heatmap of the hierarchical clustering analysis of DEGs from the salt-tolerant Jc183, and the respective expressions by the salt-sensitive Jc171 accession, after 3 h of salt exposure (150 mM NaCl). The *input* data corresponded the ratio of Log_2FC (Fold Change) values, comparing the abundances of the transcript in the stressed library with the negative control library. DEGs: differentially expressed genes [*p-value* ≤ 0.0001; false discovery rate, FDR ≤ 0.005; Log_2 (FC) ≥ 1 (up-regulation, red) or ≤ -1 (down-regulation, green). The asterisks identify DEGs selected to the RT-qPCR analysis.

- lipid metabolism (Fig. 4D): 33 unigenes related to lipid synthesis or degradation; the triacylglycerol lipase (bin 11.9.2.1) was associated with UR DEG (both accessions), while the UDP-glucose:sterol glucosyltransferase (bin 11.8.3) modulated differentially, according to the accession (Jc171/DR, and Jc183/UR);
- redox metabolism (Fig. 4E): 34 unigenes mostly related to thioredoxin, glutaredoxin, ascorbate, glutathione, dismutase, and catalase; the unigene for ascorbate (bin 21.2.2) modulated differentially, according to the accession (Jc171/UR; Jc183/DR);
- secondary metabolism (Fig. 4F): 25 unigenes mostly associated with isoprenoids, flavonoids, phenylpropanoids, and lignin biosynthesis; the phenylalanine ammonia-lyase (PAL, bin 16.2.1.1), represented by UR DEG (Jc183), was also selected to the RT-qPCR assay.

3.7. The differentially expressed unigenes validated through RT-qPCR analysis

We selected nine DEGs from the salt-tolerant Jc183 profile (Fig. 5) to the RT-qPCR assay, including two UR DEGs nearly not modulated by Jc171 [phenylalanine ammonia-lyase (*PAL*), and S-adenosylmethionine-dependent methyltransferase (*SAMe*)], six declared DEGs, also from the Jc171 profile [S-adenosylmethionine synthase (*SAM*), peroxidase (*PX*), carboxylesterase (*CXE*), homeobox-leucine zipper gene (*HD-ZIP*), NAC transcript factor gene (*NAC*), and methionine-gamma lyase (*MGL*)], and one Jc183 DR DEG (xyloglucan endotransglucosylase, *XTH*). Concerning these targets, the proposed primer pairs successfully amplified amplicons with the cDNAs samples (Fig. S2), except for the *PX* primers with Jc171 cDNA. The proposed primer pairs showed acceptable values for amplification efficiency (E), *slope* (s), and correlation coefficient (R) (Fig. S3). The RT-qPCR results (Table 1) confirmed most of the observed *in silico* expression data (Table 2).

4. Discussion

Regarding the two Brazilian *J. curcas* accessions assessed in this study, and according to Lozano-Isla et al. (2018), the CNPAE183 accession (henceforth, Jc183, for brevity) is more salt-tolerant than the JCAL171 (Jc171) accession. When cultivated without salt in greenhouse during the experimental assay, plants of these accessions were considered in a steady-state condition, consequently not stressed by environmental factors of daytime air temperature, vapor pressure deficit (VPD), and integrated global radiation (data with variation near the average data). Thus, if the transcriptomic analyses of the accessions after the salt-treatment showed significant transcriptional modulations, these changes could result from the salt stimulus. Phenotypically, 3 h after the salt exposure (150 mM NaCl), leaves of Jc171 (the salt-sensitive accession) started to show visible symptoms (wilting, dehydration, and necrosis). Similar visible damages (wilting and leaves dehydration) on *G. hirsutum* leaves of the cotton salt-sensitive Nan Dan Ba Di Da Hua genotype were associated with the saline stress (200 mM NaCl) 0.5 h after the salt-treatment, while 4 h after it, wilting was more severe (Peng et al., 2014). Furthermore, Walia et al. (2005) found necrosis on about one-third the length in leaves of the sensitive rice cultivar IR29 showed after a declared moderate salt stress exposition (NaCl and $CaCl_2$ in a 5:1 M concentration). The above-mentioned damages could compromise the photosynthesis, growth, and development of plants, and consequently their yields. In an attempt to minimize potential damages, plants under salt stress reprogram their transcriptomes. In this study, an expressive gene modulation of the salt-sensitive Jc171 accession appeared upon the salt-stimulus in comparison to the salt-tolerant Jc183 accession. Similarly, upon a saline stress treatment (Walia et al., 2005), the salt-sensitive rice IR29 induced a relatively large number of probe sets through a GeneChip analysis on the rice genome Affymetrix array in relation to the salt-tolerant FL478 genotype. The same profile appeared in another assay (Walia et al., 2007) with the same GeneChip, which analyzed other two *japonica* rice lines in addition to the two *indica* rice lines previously mentioned (Agami and M103).

The different numbers of DEGs in the accessions, in addition to the distinguished genotypes assessed, also derive from the saline treatment (salt and its molarity), salt exposure time, and the method/thresholds applied in the statistical analysis. A comparison between this study and Zhang et al. (2014) using *J. curcas* plants of similar development stage, reveals a higher NaCl solution molarity applied in our (150 *versus* 100 mM), and more stringent DEG thresholds (*p-value* ≤ 0.0001, FDR ≤ 0.005, Log_2 FC ≥ 1 or ≤ -1) in relation to that discriminating the tags ($p < 0.01$, and FC ≥ 1.8). However, despite the different DEG numbers, both accessions/profiles could contribute to understand the *J. curcas* salt-responses and identify salt-tolerance genes. Considering the potential chimeric assembled sequences found by aligning the assembled transcripts to the reference genome (partial alignments mapped to different strands/different chromosomes/in reverse order/too far away), the assembly quality of the proposed *de novo* transcriptome proved acceptable, having pointed to only 609 possible chimeric sequences (0.72 %). Additionally, because of the reference genome fragmentation (6,024 scaffolds), those sequences could even be false chimeric. Regarding the annotation process of the assembled transcripts, despite the availability of 27,661 *J. curcas* proteins from the UniProtKB database (January 2019), they are mostly (24,288) described as *uncharacterized proteins*. Thus, including proteome data from *R. communis* and *M. esculenta*, two taxonomic related species increased their annotation efficiency, especially with *R. communis* from the Phytozome database.

4.1. Metabolic responses of the accessions to the salt stimulus

In addition to the relatively high intense transcriptional effort of Jc171 compared to the Jc183 accession, the clusters of co-expressed unigenes associated with the MapMan categories showed more induced/up-expressed unigenes than the repressed/down-expressed ones. Similarly, a transcriptomic study by Walia et al. (2007) also revealed a strikingly large number of genes induced by the sensitive rice lines (IR29 and M103) than the tolerant ones considering their respective saline stress responses.

The induced unigenes found associated with several phytohormones, including ABA, ETH, AUX, JA, BR, GA, and salicylic acid (SA), highlighted the expected multiple interactions in the phytohormone network interfering with regulatory proteins and the signal transduction pathways in plants responding to salt stimulus. The root growth in plants under osmotic stress is regulated by ABA via an interacting hormonal network with AUX and ETH, in addition to cytokinin (CK) (Rowe et al., 2016). Thus, during osmotic stress, some phytohormones are positively affected [ABA, JA, and 12-OPDA (JA-precursor 12-oxo-phytodienoic acid)], while others are involved in a negative or repressed way (e.g., gibberellin - GA). This study detected some down-expressed CK-related unigenes (DR Jc171 DEGs) that were not modulated by the Jc183 accession. *Arabidopsis* CK-deficient plants showed enhanced salt- (250 mM NaCl) and drought-tolerance, and the CK-downregulation related to the cell membrane integrity and ABA hypersensitivity (Nishiyama et al., 2011). Moreover, despite their close relation, the phytohormones AUX and CK have some opposite actions. They influence the development of the root system architecture (RSA), comprised of the main root and the lateral roots, in dicotyledonous plants under normal conditions (Guan et al., 2014). Under salt stress, RSA development is also influenced by ABA, JA, ETH, and BR (Julkowska and Testerink, 2015). Upon salt stimulus, the endogenous ABA level increases due to dioxygenases cleaving carotenoid precursors (Julkowska and Testerink, 2015). In this study, the unigene induced for 9-cis-epoxycarotenoid-dioxygenase (EC 1.13.11.51) could increase the ABA synthesis. Additionally, an accumulated ABA could assist the plant acclimatization under stress, contributing to the stomatal closure, growth modulation, and synthesis of protective metabolites, including osmoprotectant compounds (e.g., proline, sugars, *myo*-inositol,

Table 1
Relative gene expression of selected unigenes from the *Jatropha curcas* L. accessions after 3 h of NaCl exposition (150 mM), according to the RT-qPCR data analyzed with the REST software (v.2.0.13).

Accession	Gene	Reaction efficiency	Gene expression	Std. Error	95 % C.I.	P(H1)	Result
Jc183	β-tubulin*	0.96	0.45				
	Actin*	0.90	2.22				
	NAC transcript factor protein (*NAC*)	1.00	28.55	7.3 - 102.3	3.1 - 430.1	0	UP
	Carboxylesterase (*CXE*)	0.97	36.79	3.8 - 421.3	2.9 - 2175.8	0	UP
	Phenylalanine ammonia-lyase (*PAL*)	0.92	9.73	1.1 - 212.4	0.1 - 583.6	0.027	UP
	β-tubulin*	0.96	0.49				
	Actin*	0.90	2.04				
	Peroxidase (*PX*)	1.00	37.19	0.6 - 3326.4	0.2 - 29,946.6	0.012	UP
	Homeobox-leucine zipper domain protein (*HD-Zip*)	0.96	5.03	0.8 - 28.4	0.2 - 77.2	0.017	UP
	Methionine gamma-lyase (*MGL*)	0.98	15.71	0.5 - 135.3	0.3 - 3093.5	0.013	UP
	β-tubulin*	0.96	0.62				
	Actin*	0.90	1.61				
	Xyloglucan endotransglucosylase/hydrolase (*XTH*)	1.00	0.19	0.1 - 0.7	0.0 - 2.1	0.002	DOWN
	S-adenosylmethionine-dependent methyltransferase (*SAMe*)	0.97	0.60	0.1 - 5.1	0.0 - 45.7	0.484	
	β-tubulin*	0.96	0.42				
	Actin*	0.90	2.40				
	S-Adenosyl-L-methionine synthase (*SAM*)	0.92	10.85	1.0-102.5	0.4-1,153.0	0.020	UP
Jc171	β-tubulin*	0.96	1.32				
	Actin*	0.90	0.76				
	NAC transcript factor protein	1.00	6.12	2.5 - 14.0	1.0 - 18.3	0	UP
	Carboxylesterase (*CXE*)	0.97	2.94	1.3 - 7.6	0.8 - 11.2	0.004	UP
	Phenylalanine ammonia-lyase (*PAL*)	0.92	2.65	0.8 - 8.0	0.4 - 10.3	0.046	UP
	β-tubulin*	0.96	1.28				
	Actin*	0.90	0.78				
	Peroxidase (*PX*)	0.96	12.13	4.6 - 36.6	3.0 - 81.7	0	UP
	Homeobox-leucine zipper domain protein (*HD-Zip*)						
	β-tubulin*	0.96	0.81				
	Actin*	0.90	1.23				
	Methionine gamma-lyase (*MGL*)	0.98	8.16	4.0 - 18.8	2.9 - 35.6	0	UP
	β-tubulin*	0.96	1.28				
	Actin*	0.90	0.78				
	Xyloglucan endotransglucosylase/hydrolase (*XTH*)	1.00	0.21	0.1 - 0.5	0.0 - 0.7	0	DOWN
	β-tubulin*	0.96	0.81				
	Actin*	0.90	1.23				
	S-adenosylmethionine-dependent methyltransferase (*SAMe*)	0.97	0.95	0.2 - 4.0	0.0 - 6.9	0.930	
	β-tubulin*	0.96					
	Actin*	0.90					
	S-Adenosylmethionine synthase (*SAM*)	0.92	1.19	0.9 - 1.7	0.7 - 2.0	0.200	

* Reference genes: Actin (Tang et al., 2016), and β-tubulin (Xu et al., 2016). UP: up-expressed; DOWN: down-expressed; P(H1): probability of the alternate hypothesis (that the between the sample and control groups is due only to chance).

polyamines), benefiting the ionic adjustment. Furthermore, because of stomatal closure and photosynthesis inhibition, plants under salt stress have lower CO_2 fixation. In this case, related to the CHO metabolism, the sucrose-phosphate synthase, one of the main enzymes in sucrose synthesis, was associated with down-expressed DEG from the Jc171 accession. In turn, the starch synthase, associated with up-expressed DEG from both accessions, could increase starch, an osmoprotectant compound protecting macromolecules (membranes and proteins) from denaturing conditions (Singh et al., 2015). Similarly, induced DEGs (from both accessions) were associated with oligosaccharides of the raffinose family and *myo*-inositols, compounds that are also osmoprotectants, which benefits the ionic adjustment.

A positive feature to withstand salinity stress is the presence of free amino acids accumulated in the cells (Zhang et al., 2019). In general, plants facing abiotic stress could increase the abundance of amino acids (Hildebrandt, 2018), including isoleucine, leucine, and valine. The unigene identified for methionine gamma-lyase (*MGL*) induced by both accessions was selected and validated through the RT-qPCR assay. MGL converts methionine to 2-ketobutyrate, a precursor in the isoleucine biosynthesis (Joshi and Jander, 2009). From the cysteine biosynthesis,

Table 2
Comparative results of gene expressions, based on the *in-silico* RNA-Seq analysis* and the RT-qPCR results**, considering the salt-tolerant (Jc183) and the salt-sensitive (Jc171) *Jatropha curcas* accessions after 3 h of NaCl exposition (150 mM).

Method/Gene Accession	*SAMe*	*PAL*	*SAM*	*PX*	*CXE*	*HD-Zip*	*NAC*	*MGL*	*XTH*
in silico#									
Jc183	3.53/UR	4.44/UR	13.50/UR	2.49/UR	2.87/UR	2.95/UR	2.76/UR	2.36/UR	−2.08/DR
Jc171	n.s.	n.s.	15.51/UR	2.76/UR	3.46/UR	5.09/UR	4.73/UR	4.99/UR	n.s.
RT-qPCR+									
Jc183	n.s.	9.73/UR	10.85/UR	37.19/UR	36.79/UR	5.03/UR	28.55/UR	15.71/UR	0.19/DR
Jc171	n.s.	2.65/ UR	n.s.	n.s.	2.94/UR	12.13/UR	6.12/UR	8.16/UR	0.21/DR

Genes: *SAMe* (S-adenosylmethionine-dependent methyltransferase); *PAL* (phenylalanine ammonia-lyase); *SAM* (S-adenosylmethionine synthase); *PX* (peroxidase); *CXE* (carboxylesterase); *HD-Zip* (homeobox- leucine zipper gene); *NAC* (NAC transcript factor gene); *MGL* (methionine-gamma lyase); *XTH* (xyloglucan endotransglucosylase); UR: up-expressed; DR: down-expressed; n.s: not significant, according the *in silico#* analysis [*p-value* ≤ 0.0001, FDR ≤ 0.005, Log_2 FC ≥ 1 (UR) or ≤ -1 (DR)] or the RT-qPCR+ results by the REST software ($p \leq$ 0.05, v.2.0.13; Pfaffl et al., 2002); FC: the ratio of the unigene abundances in the stressed in relation to the respective control library; FDR: false discovery rate.

the induced unigenes for *OASTL* and *SAT* may represent potential transgenes since plants overproducing one or both enzymes proved tolerant to abiotic stresses (Sirko et al., 2004).

Additionally, the divergences found on gene regulation found in the accessions assessed responding to salt could contribute to identify potential salt-tolerance genes. The sterol glycosyltransferase (SGT), enzyme responsible for sterol glycosylation to produce sterol glycosides, was associated with unigene showing up-expression by Jc183, and down-expression by Jc171, after salt exposure. In the lipid metabolism, the glycosylated sterols play a crucial role when associated with membrane-bound lipids modulating properties and function of membranes (Ramirez-Estrada et al., 2017). The expression of similar *SGT* gene in tomato plants (*SlSGT4*) increased the tolerant responses to osmotic, saline, and cold stresses (Ramirez-Estrada et al., 2017), while transgenic tobacco plants expressing *WsSGTL1* gene (from *Withania somnifera*) provided salt tolerance by improving the antioxidant system (Pandey et al., 2014). At the cellular level, salinity alters the ionic homeostasis by raising an imbalance in the redox status of the cells, with subsequent high production of reactive oxygen species (ROS), which is perceived by the antioxidant systems and related enzymes (Foyer and Noctor, 2009). In general, these enzymes are expected to be up-expressed. In the redox metabolism, induced unigenes (expressed by Jc171 accession) were associated with ascorbate, glutathione, ferredoxin-thioredoxin reductase, and superoxide dismutase. The induction of ascorbate-glutathione prevented the harmful production of singlet oxygen in the photosystem PSII of plants responding to salt stress (300 mM NaCl) (Wiciarz et al., 2018). In turn, the ROS-protection mechanisms also involve secondary metabolites, such as carotenoids, isoprenoids, and flavonoids (Du et al., 2015). In this study, most of the unigenes associated with isoprenoid, phenylpropanoid, and flavonoid pathways were up-expressed by the Jc171 accession responding to salt. Transcriptional changes associated with the aforementioned pathways appeared in *Medicago* root apexes responding to salt stress (100 mM NaCl) one hour after the salt treatment (Gruber et al., 2009). In the phenylpropanoid pathway, the PAL enzyme is the entry-point catalyzing the first step and not only contributing to the phytoalexin accumulation, but also benefiting plants when responding primarily to biotic stresses (Zhang et al., 2013). Our RT-qPCR results validated the induction observed by Jc183 DEG associated to PAL. For being precursors of flavonoids, which, along with terpenoids (isoprenoids) are antioxidant compounds, phenylpropanois benefit plants in salt-stress acclimatization.

According to the JA action model presented by Riemann et al. (2015), the production of JA in plants responding to salt stress leads to the degradation of the JAZ repressor, consequently releasing MYC2, which is a versatile transcription factor (TF), also activated by ABA. Additionally, with the lower bioactive GA level, DELLA proteins (which are GA repressors) accumulate and interact with JAZ, also releasing MYC2 TF from repression. MYC2 TF, in turn, activates metabolic pathways, including those related to secondary compounds, such as flavonoids and terpenoids. Curiously, salinity stress-induced genes involved in the flavonoid biosynthesis pathway appeared in the salt-sensitive rice IR29 accession, but not in the salt-tolerant FL478 (Walia et al., 2005).

4.2. The expression validation of differentially expressed unigenes by RT-qPCR assay and the development of molecular markers

Molecular markers are usually applied in genetic studies, such as genetic linkage and mapping, genetic diversity analysis, genetic quality control, and marker-assisted breeding. Among the molecular markers, microsatellite (or SSR) is one of the most informative due to its multiallelic and co-dominant features able to distinguish homozygotes from heterozygotes (Paux et al., 2012). Additionally, the *in-silico* prospection of SSR motifs from ESTs (EST-SSR) and genomes (g-SSR) available in public database involves easy application and low cost. Therefore, primers for SSR markers could benefit plant breeding programs. This study provided primer pairs successfully designed from 1,423 *J. curcas* DEGs with SSR motifs in order to develop SSR markers (Table S8). In addition, the DEGs identified in this study can represent functional (non-anonymous) molecular markers in RT-qPCR assays. Further accessions showing desirable gene expression profile can be assessed through RT-qPCR assays for the selection steps in breeding programs. The RT-qPCR results of the DEGs candidates selected from the salt-tolerant Jc183 profile are discussed below.

4.2.1. Phenylalanine ammonium lyase (PAL)

The RT-qPCR results confirmed the UR expression by Jc183 (also from Jc171, primary not detected *in-silico*); the induction of the *LjPAL* gene increased the *Lotus japonica* tolerance to saline stress (150 mM NaCl) (Mrázová et al., 2017); the PAL enzyme catalyzes the deamination of L-phenylalanine (in the phenylpropanoid pathway) providing secondary metabolites precursors (Ibrahim et al., 2019), some related to flavonoids, and anthocyanins, which had been associated with plant stress responses (Hsieh et al., 2010);

4.2.2. S-adenosylmethionine-dependent methyltransferase (SAMe)

The RT-qPCR results confirmed the n.s. expression of Jc171 (probable the salt-exposure time not sufficient); in *Ipomoea batatas* under 86 mM NaCl, the *SAMe* gene (*IbSIMT1*) was induced during the first 12 h of stress (Liu et al., 2015; Hayashi et al., 2018); additionally, semi-quantitative RT-PCR analysis showed the highest expression in *J. curcas* roots eight hours after salt exposure (150 mM NaCl, Eswaran et al., 2012); the SAMe enzyme is synthesized from ATP and methionine by the SAM enzyme (Luka et al., 2009), which was another RT-qPCR candidate;

4.2.3. S-adenosylmethionine synthase (SAM)

The RT-qPCR results confirmed the UR expression of the Jc183 accession; transgenic tobacco plants overexpressing *SAMS2* gene from *Suadea salsa* increased the PA content and improved salt-stress tolerance (200 mM NaCl) (Qi et al., 2010); the SAM enzyme catalyzes the generation of S-adenosylmethionine (Lindermayr et al., 2006), which is a polyamine (PA) precursor; PAs, such as putrescine, spermidine, and spermine are osmoprotectant compounds with roles in the osmotic adjustment of cells under salt stress (Chen et al., 2018; Baniasadi et al., 2018);

4.2.4. Carboxylesterase (CXE)

The RT-qPCR results confirmed the UR expression by both accessions; the CXE enzyme hydrolyzes esters of short-chain fatty acids (Liu et al., 2014); some potential CXE functions involved signal transduction, phytohormones activation (SA and JA), and gene regulation (Gershater and Edwards, 2007; Lord et al., 2013);

4.2.5. Homeobox-leucine zipper gene (HD-Zip)

The RT-qPCR results confirmed the UR expression of both accessions; the HD-Zip TF is involved in ABA signaling pathway (Ding et al., 2017), activating and repressing ABA-responsive genes, with relevant roles in plant growth and abiotic stress responses, including salt stress (Shen et al., 2018);

4.2.6. NAC transcription factor gene (NAC)

The RT-qPCR results confirmed the UR expression of both accessions, corroborating Zhang et al. (2014); its role as transgene was studied in transgenic rice plants under salt-treatment (150 mM NaCl; Hong et al., 2016); NAC (NAM, AFAT, and CUC; Shao et al., 2015) TF protein presents crucial roles in abiotic stress responses as transcriptional activator modulating the ABA-mediated pathway in salt-stress tolerance (Mao et al., 2015; Sakuraba et al., 2015); it is also associated with the synthesis and accumulation of proline and osmoprotectant sugars (Song et al., 2011);

4.2.7. Methionine-gamma lyase (MGL)

The RT-qPCR results confirmed the UR expression of both accessions; MGL degrades L-methionine generating α-ketobutyrate, which is a precursor of isoleucine, essential amino acid and also osmoprotectant compound in plant cells under salt stress (Farhangi-Abriz and Ghassemi-Golezani, 2016);

4.2.8. Peroxidase (PX)

The RT-qPCR results confirmed the UR expression by Jc183 accession, while there was not amplification with Jc171 cDNA; the enzyme (oxidoreductase) catalyzes the reduction of peroxides, such as hydrogen peroxide (H_2O_2; Chanwun et al., 2013); the PX-ROS interaction is notable in cellular detoxification and ROS scavenging (Schaffer and Bronnikova, 2012);

4.2.9. Xyloglucan endotransglucosylase (XTH)

The RT-qPCR results confirmed the DR expression of Jc183 accession and indicated the same for Jc171 (not detect *in-silico*); differently, induced candidate appeared in *J. curcas* plants two hours after exposure to salt stress (Wang et al., 2014), while the transgene *CaXTH* (*Capsicum annuum*) was induced in *Arabidopsis* plants six days after the salt treatment (100 mM NaCl, Cho et al., 2006); the XTH enzyme is involved in wall remodeling and cell expansion (Tenhaken, 2015).

5. Conclusion

The *de novo* RNA-Seq transcriptome based on two Brazilian *J. curcas* accessions responding to salinity (150 mM NaCl, three hours after the exposure) proved adequately assembled, with few potential chimeric sequences, and a relevant data novelty involving transcripts without acceptable similarities to the applied reference sequences. The RNA-Seq analysis pointed to the salt-sensitive Jc171 accession inducing more DEGs than the salt-tolerant Jc183 in response to the salt stimulus. Based on DEGs covering several metabolisms (phytohormone, CHO, lipid, amino acid, redox, and secondary), the up-expression of DEGs numerically exceeded the down-expression ones (by both accessions). The lower gene modulation expressed by the salt-tolerant Jc183 accession suggested a better plant-acclimatization during the first three hours after the salt stimulus, probable taking advantage of some protective strategies by trying to stabilize photosystems, protect membranes and proteins, modulate the redox state, and provide detoxification of free radicals. Thus, the validated DEGs, selected from the Jc183 profile reinforced the roles of protective strategies, combining phytohormone signaling (*CXE*, *NAC TF*, *HD-ZIP TF*), ROS detoxification (*SAMe*, *PX*), and osmoprotectant-related compounds (*PAL*, *SAM*, *MGL*). DEGs could be explored as functional molecular markers, amplifying expected qPCR profiles from cDNAs samples of stressed plants, helping marker-assisted selection steps in *J. curcas* breeding programs. Furthermore, DEGs with identified SSR motifs could be useful to develop SSR molecular markers seeking to explore polymorphisms associated with the differentially expressed sequences. However, further studies are necessary to fully elucidate the molecular basis involving salt-responsive plants and help improving the development of *J. curcas* salt-tolerant plants.

CRediT authorship contribution statement

Marislane Carvalho Paz de Souza: Formal analysis, Investigation, Validation, Writing - original draft. **Manassés Daniel da Silva:** Formal analysis, Investigation, Validation. **Eliseu Binneck:** Methodology, Software, Data curation. **George André de Lima Cabral:** Formal analysis, Investigation. **Ana Maria Benko Iseppon:** Methodology, Resources. **Marcelo Francisco Pompelli:** Funding acquisition, Project administration, Methodology, Formal analysis. **Laurício Endres:** Funding acquisition, Project administration, Methodology, Formal analysis. **Éderson Akio Kido:** Conceptualization, Methodology, Resources, Writing - original draft, Writing - review & editing.

Declaration of Competing Interest

The authors declare that there are no conflicts of interest.

Acknowledgements

The authors would like to thank the *Empresa Brasileira de Pesquisa Agropecuária* (EMBRAPA SOJA, Londrina, PR – Brazil) and the *Universidade Federal de Alagoas* (UFAL) for proving us with their facilities. This study received the support of the following Brazilian institutions (grants and fellowships): *Universidade Federal de Pernambuco* (UFPE), *Fundação de Amparo à Ciência e Tecnologia do Estado de Pernambuco* (FACEPE), *Coordenação de Aperfeiçoamento de Pessoal de Nível Superior* (CAPES), and *Conselho Nacional de Desenvolvimento Científico e Tecnológico* (CNPq: 404357/2013-0, and 311894/2017-8).

Appendix A. Supplementary data

Supplementary material related to this article can be found, in the online version, at doi:https://doi.org/10.1016/j.indcrop.2020.112168.

References

Baniasadi, F., Saffari, V.R., Moud, A.A.M., 2018. Physiological and growth responses of *Calendula officinalis* L. plants to the interaction effects of polyamines and salt stress. Sci. Hortic. 234, 312–317. https://doi.org/10.1016/j.scienta.2018.02.069.

Beltrão, N.D.M., Oliveira, M.I.P., 2008. Oleaginosas e seus óleos: vantagens e desvantagens para produção de biodiesel. Embrapa Algodão-Documentos (INFOTECA-E).

Bolger, A.M., Lohse, M., Usadel, B., 2014. Trimmomatic: a flexible trimmer for Illumina sequence data. Bioinformatics 30, 2114–2120. https://doi.org/10.1093/bioinformatics/btu170.

Bryant, D.M., Johnson, K., Di Tommaso, T., Tickle, T., Couger, M.B., Payzin-Dogru, D., Lee, T.J., Leigh, N.D., Kuo, T.H., Davis, F.G., Bateman, J., Bryant, S., Guzikowski, A.R., Tsai, S.L., Coyne, S., Ye, W.W., Freeman, R.M., Peshkin, L., Tabin, C.J., Regev, A., Haas, B.J., Whited, J.L., 2017. A tissue-mapped axolotl de novo transcriptome enables identification of limb regeneration factors. Cell Rep. 18, 762–776. https://doi.org/10.1016/j.celrep.2016.12.063.

Bushmanova, E., Antipov, D., Lapidus, A., Suvorov, V., Prjibelski, A.D., 2016. rnaQUAST: a quality assessment tool for *de novo* transcriptome assemblies. Bioinformatics 32 (14), 2210–2212. https://doi.org/10.1093/bioinformatics/btw218.

Bustin, S.A., Benes, V., Garson, J.A., Hellemans, J., Huggett, J., Kubista, M., Vandesompele, J., 2009. The MIQE guidelines: minimum information for publication of quantitative real-time PCR experiments. Clin. Chem. 55, 611–622. https://doi.org/10.1373/clinchem.2008.112797.

Cartagena, J.A., Seki, M., Tanaka, M., Yamauchi, T., Sato, S., Hirakawa, H., Tsuge, T., 2015. Gene expression profiles in *Jatropha* Under drought stress and during recovery. Plant Mol. Biol. Rep. 33, 1075–1087. https://10.1007/s11105-014-08150.

Chanwun, T., Muhamad, N., Chirapongsatonkul, N., Churngchow, N., 2013. *Hevea brasiliensis* cell suspension peroxidase: purification, characterization and application for dye decolorization. AMB Express 3, 14. https://doi.org/10.1186/2191-0855-3-14.

Chen, D., Shao, Q., Yin, L., Younis, A., Zheng, B., 2018. Polyamine function in plants: metabolism, regulation on development, and roles in abiotic stress responses. Front. Plant Sci. 9, 1945. https://doi.org/10.3389/fpls.2018.01945.

Cho, S.K., Kim, J.E., Park, Jong-A.P., Eom, T.J., Kim, W.T., 2006. Constitutive expression of abiotic stress-inducible hot pepper CaXTH3, which encodes a xyloglucan endotransglucosylase/hydrolase homolog, improves drought and salt tolerance in transgenic *Arabidopsis* plants. FEBS Lett. 580, 3136–3144. https://doi.org/10.1016/j.febslet.2006.04.062.

Ding, Z., Fu, L., Yan, Y., Tie, W., Xia, Z., Wang, W., Peng, M., Hu, W., Zhang, J., 2017. Genome-wide characterization and expression profiling of HD-Zip gene family related to abiotic stress in cassava. PLoS One. https://doi.org/10.1371/journal.pone.0173043.

Du, B., Jansen, K., Kleiber, A., Eiblmeier, M., Kammerer, B., Ensminger, I., Gessler, A., Rennenberg, H., Kreuzwieser, J., 2015. A coastal and an interior Douglas fir provenance exhibit different metabolic strategies to deal with drought stress. Tree Physiol. 36, 148–163. https://doi.org/10.1093/treephys/tpv105.

Eswaran, N., Parameswaran, S., Anantharaman, B., Raja Krishna Kumar, G., Sathram, B., Johnson, T.S., 2012. Generation of an expressed sequence tag (EST) library from salt-stressed roots of *Jatropha curcas* for identification of abiotic stress-responsive genes. Plant Biol. 14, 428–437. https://doi.org/10.1111/j.1438-8677.2011.00529.x.

Disponível em:https://www.fao.org/docrep/003/T0234E/T0234E00.htm. Acesso em 15 de Dez de 2018.

Farhangi-Abriz, S., Ghassemi-Golezani, K., 2016. Improving amino acid composition of soybean under salt stress by salicylic acid and jasmonic acid. J. Appl. Bot. Food Qual. 89, 243–248. https://doi.org/10.5073/JABFQ.2016.089.031.

Foyer, C.H., Noctor, G., 2009. Redox regulation in photosynthetic organisms: signaling, acclimation, and practical implications. Antioxid. Redox Signaling 11, 861–905. https://doi.org/10.1089/ars.2008.2177.

Gershater, M.C., Edwards, R., 2007. Regulating biological activity in plants with

carboxylesterases. Plant Sci. 173 (6), 579–588. https://doi.org/10.1016/j.plantsci.2007.08.008.
Grabherr, M.G., Haas, B.J., Yassour, M., Levin, J.Z., Thompson, D.A., Amit, I., Adiconis, Z., Fan, L., Raychowdhury, R., Zeng, Q., Chen, Z., Mauceli, E., Hacohen, N., Gnirke, A., Rhind, N., Di Palma, F., Birren, B.W., Nusbaum, C., Lindblad-Toh, K., Friedman, N., Regev, A., 2011. Full-length transcriptome assembly from RNA-seq data without a reference genome. Nat. Biotechnol. https://doi.org/10.1038/nbt.1883.
Grover, A., Kumari, M., Singh, S., Rathode, S.S., Gupta, S.M., Pandey, P., Gilotra, S., Kumar, D., Arif, M., Ahmed, Z., 2014. Analysis of *Jatropha curcas* transcriptome for oil enhancement and genic markers. Physiol. Mol. Biol. Plants 20, 139–142. https://doi.org/10.1007/s12298-013-0204-4.
Gruber, V., Blanchet, S., Diet, A., Zahaf, O., Boualem, A., Kakar, K., Alunni, B., Udvardi, M., Frugier, F., Crespi, M., 2009. Identification of transcription factors involved in root apex responses to salt stress in *Medicago truncatula*. Mol. Genet. Genomics 281, 55–66. https://doi.org/10.1007/s00438-008-0392-8.
Guan, C., Wang, X., Feng, J., Hong, S., Liang, Y., Ren, B., Zuo, J., 2014. Cytokinin antagonizes abscisic acid-mediated inhibition of cotyledon greening by promoting the degradation of abscisic acid insensitive5 protein in *Arabidopsis*. Plant Physiol. 3, 1515–1526. https://doi.org/10.1104/pp.113.234740.
Hayashi, T., Teruya, T., Chaleckis, R., Morigasaki, S., Yanagida, M., 2018. S-Adenosylmethionine synthetase is required for cell growth, maintenance of G0 phase, and termination of quiescence in fission yeast. iScience 5, 38–51. https://doi.org/10.1016/j.isci.2018.06.011.
Hildebrandt, T.M., 2018. Synthesis versus degradation: directions of amino acid metabolism during *Arabidopsis* abiotic stress response. Plant Mol. Biol. 98, 121–135. https://doi.org/10.1007/s11103-018-0767-0.
Hoagland, D.R., Arnon, D.I., 1950. The Water Culture Method for Growing Plants Without Soil. California agricultural Experimental Station Circular No. 347. University of California, Berkeley, pp. 1–32.
Hong, Y., Zhang, H., Huang, L., Li, D., Song, F., 2016. Overexpression of a stress-responsive NAC transcription factor gene ONAC022 improves drought and salt tolerance in rice. Front. Plant Sci. 7, 4. https://doi.org/10.3389/fpls.2016.00004.
Hsieh, L.S., Ma, G.J., Yang, C.C., Lee, P.D., 2010. Cloning, expression, site-directed mutagenesis and immunolocalization of phenylalanine ammonia-lyase in *Bambusa oldhamii*. Phytochemistry 71, 1999–2009. https://doi.org/10.1016/j.phytochem.2010.09.019.
Ibrahim, W., Zhu, Y.M., Chen, Y., Qiu, C.W., Zhu, S., Wu, F., 2019. Genotypic differences in leaf secondary metabolism, plant hormones and yield under alone and combined stress of drought and salinity in cotton genotypes. Physiol. Plant. 165, 343–355. https://doi.org/10.1111/ppl.12862.
Julkowska, M.M., Testerink, C., 2015. Tuning plant signaling and growth to survive salt. Trends Plant Sci. 9, 586–594. https://doi.org/10.1016/j.tplants.2015.06.008.
Juntawong, P., Sirikhachornkit, A., Pimjan, R., Sonthirod, C., Sangsrakru, D., Yoocha, T., Tangphatsornruang, S., Srinives, P., 2014. Elucidation of the molecular responses to waterlogging in *Jatropha* roots by transcriptome profiling. Front. Plant Sci. https://doi.org/10.3389/fpls.2014.00658.
Langmead, B., Trapnell, C., Pop, M., Salzberg, S.L., 2009. Ultrafast and memory- efficient alignment of short DNA sequences to the human genome. Genome Biol. 10, R25. https://doi.org/10.1186/gb-2009-10-3-r25.
Li, B., Dewey, C., 2011. RSEM: accurate transcript quantification from RNA-Seq data with or without a reference genome. BMC Bioinformatics 12, 323. https://doi.org/10.1186/1471-2105-12-323.
Lindermayr, C., Saalbach, G., Bahnweg, G., Durner, J., 2006. Differential inhibition of *Arabidopsis* methionine adenosyltransferases by protein S-nitrosylation. J. Biol. Chem. 281, 4285–4291. https://doi.org/10.1074/jbc.M511635200.
Liu, D., Wang, L., Zhai, H., Song, X., He, S., Liu, Q., 2014. A novel α/β-hydrolase gene IbMas enhances salt tolerance in transgenic sweetpotato. PLoS One 9, e115128. https://doi.org/10.1371/journal.pone.0115128.
Liu, D., He, S., Song, X., Zhai, H., Liu, N., Zhang, D., Liu, Q., 2015. IbSIMT1, a novel salt-induced methyltransferase gene from *Ipomoea batatas*, is involved in salt tolerance. Plant Cell Tissue Organ Cult. 120, 701–715. https://doi.org/10.1007/s11240-014-0638-6.
Lord, C.C., Thomas, G., Brown, J.M., 2013. Mammalian alpha beta hydrolase domain (ABHD) proteins: lipid metabolizing enzymes at the interface of cell signaling and energy metabolism. Biochim. Biophys. Acta (BBA) – Mol. Cell Biol. L. 1831, 792–802. https://doi.org/10.1016/j.bbalip.2013.01.002.
Lozano-Isla, F., Campos, M.L.O., Endres, L., Bezerra-Neto, E., Pompelli, M.F., 2018. Eff ;ects of seed storage time and salt stress on the germination of *Jatropha curcas* L. Ind. Crops Prod. 118, 214–224. https://doi.org/10.1016/j.indcrop.2018.03.052.
Luka, Z., Mudd, S.H., Wagner, C., 2009. Glycine N-methyltransferase and regulation of S-adenosylmethionine levels. J. Biol. Chem. 284, 22507–22511. https://doi.org/10.1074/jbc.R109.019273.
Mao, H., Wang, H., Liu, S., Li, Z., Yang, X., Yan, J., Li, J., Lam-Son, P.T., Qin, F., 2015. A transposable element in a NAC gene is associated with drought tolerance in maize seedlings. Nat. Commun. 6, 8326. https://doi.org/10.1038/ncomms9326.
Mrázová, A., Belay, S.A., Eliášová, A., Perez-Delgado, C., Kaducová, M., Betti, M., Vega, J.M., Paľove-Balang, P., 2017. Expression, activity of phenylalanine-ammonia-lyase and accumulation of phenolic compounds in Lotus japonicus under salt stress. Biologia 72, 36–42. https://doi.org/10.1515/biolog-2017-0001.
Munns, R., 2005. Genes and salt tolerance: bringing them together. New Phytol. 167, 645–663. https://doi.org/10.1111/j.1469-8137.2005.01487.x.
Nishiyama, R., Watanabe, Y., Fujita, Y., Le, D.T., Kojima, M., Werner, T., Vankova, R., Yamaguchi-Shinozaki, K., Shinozaki, K., Kakimoto, T., Sakakibara, H., Schmülling, T., Tran, L.S., 2011. Analysis of cytokinin mutants and regulation of cytokinin metabolic genes reveals important regulatory roles of cytokinins in drought, salt and abscisic acid responses, and abscisic acid biosynthesis. Plant Cell 23, 2169–2183. https://doi.org/10.1105/tpc.111.087395.
Oliveros, J.C., 2015. Venny. An Interactive Tool for Comparing Lists With Venn's Diagrams. https://bioinfogp.cnb.csic.es/tools/venny/index.html.
Pandey, V., Niranjan, A., Atri, N., Chandrashekhar, K., Mishra, M.K., Trivedi, P.K., Misra, P., 2014. WsSGTL1 gene from *Withania somnifera*, modulates glycosylation profile, antioxidant system and confers biotic and salt stress tolerance in transgenic tobacco. Planta 6, 1217–1231. https://doi.org/10.1007/s00425-014-2046-x.
Paux, E., Sourdille, P., Mackay, I., Feuillet, C., 2012. Sequence-based marker development in wheat: advances and applications to breeding. Biotechnol. Adv. 30, 1071–1088. https://doi.org/10.1016/j.biotechadv.2011.09.015.
Peel, M.C., Finlayson, B.L., McMahon, T.A., 2007. Updated world map of the Köppen-Geiger climate classification. Hydrol. Earth Syst. Sci. Discuss. 11, 1633–1644. https://doi.org/10.5194/hess-11-1633-2007.
Peng, Z., He, S., Gong, W., Sun, J., Pan, Z., Xu, F., Lu, Y., Du, X., 2014. Comprehensive analysis of differentially expressed genes and transcriptional regulation induced by salt stress in two contrasting cotton genotypes. BMC Genomics 15, 760. https://doi.org/10.1186/1471-2164-15-760.
Pfaffl, M.W., Horgan, G.W., Dempfle, L., 2002. Relative expression software tool (REST©) for group-wise comparison and statistical analysis of relative expression results in real-time PCR. Nucleic Acids Res. 30, e36. https://doi.org/10.1093/nar/30.9.e36.
Pramanik, K., 2003. Properties and use of *Jatropha curcas* oil and diesel fuel blends in compression ignition engine. Renew. Energy 28, 239–248. https://doi.org/10.1016/S0960-1481(02)00027-7.
Proclima, 2019. Water Balance in the Municipality of Maceió, AL, Brazil. in, Vol 2019. National Institute for Space Research, São José dos Campos. Available on https://proclima.cptec.inpe.br/. Accessed on July 19, 2019.
Qi, Y.C., Wang, F.F., Zhang, H., Liu, W.Q., 2010. Overexpression of *Suadea salsa* S-adenosylmethionine synthetase gene promotes salt tolerance in transgenic tobacco. Acta Physiol. Plant. 32, 263–269. https://doi.org/10.1007/s11738-009-0403-3.
Ramirez-Estrada, K., Castillo, N., Lara, J.A., Arró, M., Boronat, A., Ferrer, A., Altabella, T., 2017. Tomato UDP-Glucose sterol glycosyltransferases: a family of developmental and stress regulated genes that encode cytosolic and membrane-associated forms of the enzyme. Front. Plant Sci. https://doi.org/10.3389/fpls.2017.00984.
Riemann, M., Dhakarey, R., Hazman, M., Miro, B., Kohli, A., Nick, P., 2015. Exploring jasmonates in the hormonal network of drought and salinity responses. Front. Plant Sci. 6, 1077. https://doi.org/10.3389/fpls.2015.01077.
Robinson, M.D., McCarthy, D.J., Smyth, G.K., 2010. edgeR: a Bioconductor package for differential expression analysis of digital gene expression data. Bioinformatics 26, 139–140. https://doi.org/10.1093/bioinformatics/btp616.
Rowe, J.H., Topping, J.F., Liu, J., Lindsey, K., 2016. Abscisic acid regulates root growth under osmotic stress conditions via an interacting hormonal network with cytokinin, ethylene and auxin. New Phytol. 1, 225–239. https://doi.org/10.1111/nph.13882.
Rozen, S., Skaletsky, H., 2000. Primer3 on the WWW for general users and for biologist programmers. Methods Mol. Biol. 132, 365–386. https://doi.org/10.1385/1-59259-192-2:365.
Sakuraba, Y., Kim, Y.S., Han, S.H., Lee, B.D., Paek, N.C., 2015. The Arabidopsis transcription factor NAC016 promotes drought stress responses by repressing AREB1 transcription through a trifurcate feed-forward regulatory loop involving NAP. Plant Cell 27, 1771–1787. https://doi.org/10.1105/tpc.15.00222.
Saldanha, A.J., 2004. Java Treeview—extensible visualization of microarray data. Bioinformatics 20, 3246–3248. https://doi.org/10.1093/bioinformatics/bth349.
Sapeta, H., Lourenço, T., Lorez, S., Grumaz, C., Kirstahler, P., Barros, P.M., Costa, J.M., Sohn, K., Oliveira, M.M., 2015. Transcriptomics and physiological analyses reveal co-ordinated alteration of metabolic pathways in *Jatropha curcas* drought tolerance. J. Exp. Bot. 67, 845–860. https://doi.org/10.1093/jxb/erv499.
Schaffer, W.M., Bronnikova, T.V., 2012. Peroxidase-ROS interactions. Nonlinear Dyn. 68, 413. https://doi.org/10.1007/s11071-011-0314-x.
Shao, H., Wang, H., Tang, X., 2015. NAC transcription factors in plant multiple abiotic stress responses: progress and prospects. Front. Plant Sci. 6, 902. https://doi.org/10.3389/fpls.2015.00902.
Shen, W., Li, H., Teng, R., Wang, Y., Wang, W., Zhuang, J., 2018. Genomic and transcriptomic analyses of HD-Zip family transcription factors and their responses to abiotic stress in tea plant (*Camellia sinensis*). Genomics. https://doi.org/10.1016/j.ygeno.2018.07.009.
Singh, A., Jha, S.K., Bagri, J., Pandey, G.K., 2015. ABA inducible rice protein phosphatase 2C confers ABA insensitivity and abiotic stress tolerance in *Arabidopsis*. PLoS One 10, e0125168. https://doi.org/10.1371/journal.pone.0125168.
Sirko, A., Błaszczyk, A., Liszewska, F., 2004. Overproduction of SAT and/or OASTL in transgenic plants: a survey of effects. J. Exp. Bot. 55, 1881–1888. https://doi.org/10.1093/jxb/erh151.
Song, S.Y., Chen, Y., Chen, J., Dai, X.Y., Zhang, W.H., 2011. Physiological mechanisms underlying OsNAC5-dependent tolerance of rice plants to abiotic stress. Planta 234, 331–345. https://doi.org/10.1007/s00425-011-1403-2.
Taiz, L., Zeiger, E., Moller, I.M., Murphy, A., 2017. Fisiologia e desenvolvimento vegetal, six ed. Artmed, Porto Alegre.
Tang, Y., Qin, S., Guo, Y., Chen, Y., Wu, P., Chen, Y., Li, M., Jiang, H., Wu, G., 2016. Genome-wide analysis of the AP2/ERF gene family in physic nut and overexpression of the JcERF011 gene in rice increased its sensitivity to salinity stress. PLoSONE 11, e0150879. https://doi.org/10.1371/journal.pone.0150879.
Tenhaken, R., 2015. Cell wall remodeling under abiotic stress. Front. Plant Sci. 5, 771. https://doi.org/10.3389/fpls.2014.00771.
Thimm, O., Blasing, O., Gibon, Y., Nagel, A., Meyer, S., Kruger, P., Selbig, J., Muller, L.A., Rhee, S.Y., Stitt, M., 2004. MAPMAN: a user – driven tool to display genomics data sets onto diagrams of metabolic pathways and other biological processes. Plant J. 37, 914–939. https://doi.org/10.1111/j.1365-313X.2004.02016.x.
Joshi, V., Jander, G., 2009. *Arabidopsis* methionine γ-Lyase is regulated according to

isoleucine biosynthesis needs but plays a subordinate role to threonine daeminase. Plant Physiol. 151, 367–378. https://doi.org/10.1104/pp.109.138651.
Walia, H., Wilson, C., Condamine, P., Liu, X., Ismail, A.M., Zeng, L., Wanamaker, S.I., Mandal, J., Xu, J., Cui, X., Close, T.J., 2005. Comparative transcriptional profiling of two contrasting rice genotypes under salinity stress during the vegetative growth stage. Plant Physiol. 139, 822–835. https://doi.org/10.1104/pp.105.065961.
Walia, H., Wilson, C., Zeng, L., Ismail, A.M., Condamine, P., Close, T.J., 2007. Genome-wide transcriptional analysis of salinity stressed japonica and indica rice genotypes during panicle initiation stage. Plant Mol. Biol. 63, 609–623. https://doi.org/10.1007/s11103-006-9112-0.
Wang, H., Zou, Z., Wang, S., Gong, M., 2013. Global analysis of transcriptome responses and gene expression profiles to cold stress of *Jatropha curcas* L. PLoS One 8, e82817. https://doi.org/10.1371/journal.pone.0082817.
Wang, H., Zou, Z., Wang, S., Gong, M., 2014. Deep sequencing-based transcriptome analysis of the oil-bearing plant Physic Nut (*Jatropha curcas* L.) under cold stress. Plant Omics 7, 178–187.
Wang, H., Gong, M., Xin, H., Tang, L., Dai, D., Gao, Y., Liu, C., 2018. Effects of chilling stress on the accumulation of soluble sugars and their key enzymes in *Jatropha curcas* seedlings. Physiol. Mol. Biol. Plants 24, 857–865. https://doi.org/10.1007/s12298-018-0568-6.
Wiciarz, M., Niewiadomska, E., Kruk, J., 2018. Effects of salt stress on low molecular antioxidants and redox state of plastoquinone and P700 in *Arabidopsis thaliana* (glycophyte) and *Eutrema salsugineum* (halophyte). Photosynthetica 56, 811–819. https://doi.org/10.1007/s11099-017-0733-0.
Xu, G., Huang, J., Yang, Y., Yao, Y.A., 2016. Transcriptome analysis of flower sex differentiation in *Jatropha curcas* L. Using RNA sequencing. PLoS One 11 (2), e0145613. https://doi.org/10.1371/journal.pone.0145613.
You, F.M., Huo, N., Gu, Y.Q., Luo, M., Ma, Y., Hane, D., Lazo, G.R., Dvorak, J., Anderson, O.D., 2008. BatchPrimer3: a high throughput web application for PCR and sequencing primer design. BMC Bioinformatics 9, 253. https://doi.org/10.1186/1471-2105-9-253.
Zhang, X., Gou, M., Liu, C.-J., 2013. *Arabidopsis* kelch repeat F-Box proteins regulate phenylpropanoid biosynthesis via controlling the turnover of phenylalanine ammonia-lyase. Plant Cell. Plant Cell 25, 4994–5010. https://doi.org/10.1105/tpc.113.119644.
Zhang, L., Zhang, C., Wu, P., Chen, Y., Li, M., Jiang, H., Wu, G., 2014. Global analysis of gene expression profiles in physic nut (*Jatropha curcas* L.) seedlings exposed to salt stress. PLoS One 9 (5), e97878. https://doi.org/10.1371/journal.pone.0097878.
Zhang, C., Zhang, L., Zhang, S., Zhu, S., Wu, P., Chen, Y., Li, M., Jiang, H., Wu, G., 2015. Global analysis of gene expression profiles in physic nut (*Jatropha curcas* L.) seedlings exposed to drought stress. BMC Plant Biol. 15, 17. https://doi.org/10.1186/s12870-014-0397-x.
Zhang, Y., Li, D., Zhou, R., Wang, X., Dossa, K., Wang, L., Zhang, Y., Yu, J., Gong, H., Zhang, X., You, J., 2019. Transcriptome and metabolome analyses of two contrasting sesame genotypes reveal the crucial biological pathways involved in rapid adaptive response to salt stress. BMC Plant Biol. 19, 66. https://doi.org/10.1186/s12870-019-1665-6.